RESEARCH ARTICLE | JULY 25 2014

Diffusive and quantum effects of water properties in different states of matter

Kuan-Yu Yeh; Shao-Nung Huang; Li-Jen Chen; Shiang-Tai Lin

J. Chem. Phys. 141, 044502 (2014)
https://doi.org/10.1063/1.4890572

Diffusive and quantum effects of water properties in different states of matter

Kuan-Yu Yeh,[1,2] Shao-Nung Huang,[1] Li-Jen Chen,[1,a)] and Shiang-Tai Lin[1,a)]
[1]*Department of Chemical Engineering, National Taiwan University, Taipei 10617, Taiwan*
[2]*Refining & Manufacturing Research Institute, CPC Corporation, Chia-Yi 60051, Taiwan*

(Received 12 March 2014; accepted 8 July 2014; published online 25 July 2014)

The enthalpy, entropy, and free energy of water are important physical quantities for understanding many interesting phenomena in biological systems. However, conventional approaches require different treatments to incorporate quantum and diffusive effects of water in different states of matter. In this work, we demonstrate the use of the two-phase thermodynamic (2PT) model as a unified approach to obtain the properties of water over the whole phase region of water from short (∼20 ps) classical molecular dynamics trajectories. The 2PT model provides an effective way to separate the diffusive modes (gas-like component) from the harmonic vibrational modes (solid-like component) in the vibrational density of states (DoS). Therefore, both diffusive and quantum effect can be properly accounted for water by applying suitable statistical mechanical weighting functions to the DoS components. We applied the 2PT model to systematically examine the enthalpy, entropy, and their temperature dependence of five commonly used rigid water models. The 2PT results are found to be consistent with those obtained from more sophisticated calculations. While the thermodynamic properties determined from different water models are largely similar, the phase boundary determined from the equality of free energy is very sensitive to the small inaccuracy in the values of enthalpy and absolute entropy. The enthalpy, entropy, and diffusivity of water are strongly interrelated, which challenge further improvement of rigid water model via parameter fitting. Our results show that the 2PT is an efficient method for studying the properties of water under various chemical and biological environments. [http://dx.doi.org/10.1063/1.4890572]

I. INTRODUCTION

Because of the fundamental importance of water in the physical and biological sciences, many experimental and theoretical studies have been devoted to understand water thermodynamic properties under different conditions and in different environments.[1–14] Computational simulations provide a detailed understanding of water properties at a molecular level that would otherwise require expensive experimental equipment to access. The calculations of enthalpy, entropy, and free energy of water from molecular simulations also provide insight into the stability of water near proteins[15,16] and nanomaterials,[17] and the phase behavior of gas hydrates.[18] Due to the unique feature of water in solid, liquid, and vapor states, different statistical mechanics-based methods have been developed to calculate enthalpy and entropy of different water phases, respectively.[19–21] For example, most commonly used free energy calculation methods (e.g., thermodynamic integration[22] and perturbation,[23] Widom's test particle insertion[24]) do not provide proper thermodynamic results based on classical simulations in the solid phase, where quantum effects are prominent.[25,26] While harmonic approximation[27] provides reasonable thermodynamic properties for solid,[28] it is not applicable to diffusive systems where particle motions are dominated by anharmonic potential surfaces. Water molecules near complex biological systems or nano-confinements might not have a clear feature of a specific state of aggregation.[7,10,17,29,30] Therefore, it would be challenging to apply conventional free energy calculation methods to study the thermodynamic properties of water in these problems.

Recently a two-phase thermodynamic (2PT) model[31–33] is developed to extract thermodynamic information of a system in any state of matter with quantum effects from the trajectory of molecular dynamic (MD) simulations. The 2PT model determines the thermodynamic properties based on the vibrational density of states (DoS), determined from the Fourier transform of the velocity autocorrelation function. In particular, a fluidicity parameter is used to decompose the DoS to a diffusive gas-like and a non-diffusive solid-like (harmonic) component. The thermodynamic properties of water are then calculated as sum of contributions from both components by applying suitable statistical weighting functions. This method allows for energy and entropy calculation of a system under all kinds of conditions. In addition, the application of quantum harmonic statistics to the solid-like component in the 2PT model allows for inclusion of quantum effects into account, which would otherwise require the much more elaborated path integral method.[34–38] The 2PT model has been shown to efficiently and accurately determine enthalpies and entropies of various types of systems, such as Lennard-Jones fluids,[31] water,[32] carbon dioxide,[39]

a)Authors to whom correspondence should be addressed. Electronic addresses: ljchen@ntu.edu.tw, Tel.: +886 (0)2 23623296, Fax: +886 (0)2 23623040 and stlin@ntu.edu.tw, Tel.: +886 (0)2 33661369, Fax: +886 (0)2 23623040.

small organic molecules,[40] metal[41] and alloys,[42] and molten salts.[43]

Herein, we systematically investigate the enthalpy (H) and entropy (S) of five commonly used rigid non-polarizable water models,[44] including TIP3P,[45] SPC/E,[46] TIP4P-Ew,[47] TIP4P-2005,[48] and TIP4P-ice,[49] in the vapor, liquid, and solid phases. The 2PT analysis allows for quantification of quantum (fraction of solid-like component) and diffusive effects (fraction of gas-like component) on the properties of water in different phases. While solid phase properties are dominated by quantum effects and gas phase properties by diffusive effects, both are important for the liquid phase. The phase boundary, especially the melting point, is rather sensitive to the balance between enthalpy and entropy, both of which are affected by quantum and diffusive effects. Our results show that the inclusion of both effects in the 2PT analysis allows for a much better thermodynamic property description of water in all phases. Therefore, the 2PT should be a useful method for studying behaviors of water and thermodynamic driving forces in complicated chemical and biological processes.

II. THEORETICAL BACKGROUND OF THE TWO-PHASE THERMODYNAMIC MODEL FOR RIGID WATER

The vibrational density of states $S(\upsilon)$, or the normal modes, of a system is represented by the mass-weighted spectral density as

$$S(\upsilon) = \frac{1}{k_B T} \sum_{l=1}^{N} \sum_{k=1}^{3} \lim_{\tau-\infty} \frac{m_l}{\tau} \left| \int_{-\tau}^{\tau} v_l^k(t) e^{-i2\pi\upsilon t} dt \right|^2, \quad (1)$$

where k_B is the Boltzmann constant, m_l is the mass of atom l, N is the total number of atoms in the systems, and v_l^k represents the velocity of l atom in the k direction ($k = x$, y, and z in Cartesian coordinate). For rigid water (polyatomic fluid), the total density of state functions can be composed into contributions from molecular translation and rotation

$$S(\upsilon) = S_{trn}(\upsilon) + S_{rot}(\upsilon), \quad (2a)$$

with translational DoS, $S_{trn}(\upsilon)$, determined from the center of mass velocities (v_l^k) of all the M water molecules

$$S_{trn}(\upsilon) = \frac{1}{k_B T} \sum_{l=1}^{\mathrm{M}} \sum_{k=1}^{3} \lim_{\tau-\infty} \frac{m_l}{\tau} \left| \int_{-\tau}^{\tau} v_l^k(t) e^{-i2\pi\upsilon t} dt \right|^2 \quad (2b)$$

and the rotational DoS, $S_{rot}(\upsilon)$, determined from the angular velocity (ω_l^k)

$$S_{rot}(\upsilon) = \frac{1}{k_B T} \sum_{l=1}^{\mathrm{M}} \sum_{k=1}^{3} \lim_{\tau-\infty} \frac{I_l^k}{\tau} \left| \int_{-\tau}^{\tau} \omega_l^k(t) e^{-i2\pi\upsilon t} dt \right|^2, \quad (2c)$$

where I_l^k is the kth principle moment of inertia of molecule l. The integration of $S(\upsilon)$ over frequency gives the total number of degree of freedom of the system. For a system of M number of water molecules, the total degree of freedom associated with translational and rotational motion is $3M$ and $3M$, respectively. Note that the zero frequency intensity, S(0), is related to the diffusivity.[32]

To the first order approximation that all the vibration modes correspond to a collection of independent harmonic oscillators, the thermodynamic properties (P) of the system can then be calculated as[31]

$$P = P_0 + \int_0^{\infty} d\upsilon S(\upsilon) W_p^{HO}(\upsilon), \quad (3)$$

where $W_p^{HO}(\upsilon)$ is the property weighting function for the corresponding thermodynamic property (e.g., $P = E$ for energy, S for entropy). If classical harmonic oscillators are considered, the weighting functions for energy and entropy are

$$W_E^{CHO}(\upsilon) = \beta^{-1}, \quad (4a)$$

$$W_S^{CHO}(\upsilon) = k_B[1 - \ln(\beta h\upsilon)], \quad (4b)$$

where $\beta = 1/k_B T$ and h is the Planck constant. In this case, the properties determined are referred to as classical one-phase thermodynamic model (classical 1PT) results. If quantum harmonic oscillators are used, these weighting functions become

$$W_E^{QHO}(\upsilon) = \frac{h\upsilon}{2} + \frac{h\upsilon}{\exp(\beta h\upsilon) - 1}, \quad (5a)$$

$$W_E^{QHO}(\upsilon) = \frac{k_b \beta h\upsilon}{\exp(\beta h\upsilon) - 1} + k_b \ln[1 - \exp(-\beta h\upsilon)]. \quad (5b)$$

The results obtained from Eqs. (3), (5a), and (5b) are referred to as quantum one-phase thermodynamic model (quantum 1PT). The difference between classical and quantum 1PT results is the quantum effects.[25] The constant P_0 in Eq. (3) is the reference value for property P. For entropy, the reference value is zero ($S_0 = 0$). For energy, the reference energy is set so that the classical results are identical to the energy obtained from MD simulation (E^{MD}), i.e.,

$$P_0 = E^{MD} - \int_0^{\infty} d\upsilon S(\upsilon) W_E^{CHO}(\upsilon) = E^{MD} - 3N\beta^{-1}. \quad (6)$$

For diffusive systems (liquid or gas), the low frequency modes are highly anharmonic and the quasiharmonic approximation of quantum 1PT becomes inadequate. For example, the nonzero frequency intensity $S(0)$ (diffusion) results in an infinitely large value of entropy (see Eq. (4b) or (5b)). To extend the method for fluids, Lin *et al.*[31] proposed to consider the DoS as a superposition of a gas-like, diffusive component and a solid-like, harmonic component, referred to as the 2PT model.

The essence of the 2PT method lies in the decomposition of DoS function into a diffusive (gas-like) and a non-diffusive (solid-like) component. According to the decomposition of DoS functions using Eq. (2a) and (2b) translational and rotational DoS functions are treated separately. The gas phase contribution associated with translational motions is assumed to be a hard sphere gas and the rotational DoS is represented as a rigid rotor. The corresponding DoS is determined by zero frequency intensity $S_i(0)$ and fluidicity (f_i) as follows:

$$S_i^g(\upsilon) = \frac{S_i(0)}{1 + \left[\frac{\pi\upsilon S_i(0)}{6 f_i M}\right]^2}, \quad (7)$$

where the subscript i denotes types of motion (translation and rotation). The fluidicity is defined as the ratio of the

self-diffusivity of the system to the hard sphere diffusivity determined in the zero pressure limit as the Chapman–Enskog result,[27] and is bounded between 0 for crystal and 1 for ideal gas. In addition, the integration of Eq. (7) gives $f_i M$, indicating the number of effective gas-like particles in the systems. Lin *et al.*[31,32] showed that under the same temperature and density, f_{trans} and f_{rot} can be calculated from

$$2\Delta_i^{-\frac{9}{2}} f_i^{\frac{15}{2}} - 6\Delta_i^{-3} f_i^5 - \Delta_i^{-\frac{3}{2}} f_i^{\frac{7}{2}} + 6\Delta_i^{\frac{-3}{2}} f_i^{\frac{5}{2}} + 2f_i - 2 = 0, \tag{8}$$

where the dimensionless diffusivity constant (Δ_i) is calculated via Eq. (9),

$$\Delta_i = \frac{2S_i(0)}{9M}\left(\frac{\pi k_B T}{m}\right)^{\frac{1}{2}}\left(\frac{N}{V}\right)^{\frac{1}{3}}\left(\frac{6}{\pi}\right)^{\frac{2}{3}}, \tag{9}$$

where V is the volume of the system and m is the mass of water molecule.

Subtracting the gas-like contribution from the total DoS function gives the solid-like DoS. The thermodynamic properties (P) are then approximated as a linear combination of properties from hard-sphere (HS)/rigid rotor and harmonic (HO) solids, i.e.,

$$P = P_0 + \sum_i^{trans,rot}\left[\int_0^\infty d\upsilon S_i^S(\upsilon) W_{i,p}^S(\upsilon) + \int_0^\infty d\upsilon S_i^g(\upsilon) W_{i,p}^g(\upsilon)\right], \tag{10}$$

where $W_{i,p}^j(\upsilon)$ is the weighting function for the corresponding thermodynamic properties (p) associated with each motion (i) of gas or solid like component.

Hard-sphere (translational) weighing functions for energy (E) and entropy (S) are described in Eqs. (11a) and (11b); free rigid rotor weighting functions are described in Eqs. (11a) and (11c),

$$W_{trans,E}^g(\upsilon) = W_{rot,E}^g(\upsilon) = 0.5, \tag{11a}$$

$$W_{trans,S}^g(\upsilon) = \frac{1}{3}\frac{S_{HS}}{k_B}, \tag{11b}$$

$$W_{rot,S}^g(\upsilon) = \frac{1}{3}\frac{S_{rot}}{k_B}, \tag{11c}$$

where S_{HS} is the hard-sphere entropy calculated using the Carnahan-Starling equation of state of hard sphere gases,[50]

$$\frac{S_{HS}}{k_B} = \frac{5}{2} + \ln\left[\left(\frac{2\pi k_B T}{h^2}\right)^{\frac{3}{2}}\frac{V}{f_{trans}N}z(y)\right] + \frac{y(3y-4)}{(1-y)^2}, \tag{12}$$

with the compressibility factor $z(y) = \frac{1+y+y^2-y^3}{(1-y)^3}$ and packing fraction $y = (f_{trans}^{5/2})/(\Delta^{3/2})$.

S_{rot} is the rotational entropy of a rigid rotor, calculated via Eq. (13),

$$\frac{S_{rot}}{k_B} = \ln\left[\frac{\pi^{1/2}e^{3/2}}{\sigma}\frac{T^3}{\theta_A\theta_B\theta_C}\right], \tag{13}$$

with θ_k being the rotational temperatures of water, and σ the rotational symmetry (2 for water). For the solid-like component, quantum harmonic weighting functions (Eqs. (5a) and (5b)) are used. The results from Eqs. (5a), (5b), and (10)–(11c) are referred to as (quantum) 2PT results. In the analysis for the phase boundary of water, we have also included the calculations from Eqs. (4a), (4b), and (10)–(11c), denoted as classical 2PT, and compared the results to classical MD simulations. The differences between 2PT and 1PT are the diffusive effects.

III. COMPUTATIONAL DETAILS

All molecular dynamics simulations were carried out with the Large-scale Atomic/Molecular Massively Parallel Simulator (LAMMPS).[51] The liquid and vapor phases are constructed in a cubic box consisting of 256 water molecules. For solid phase, a 516 water molecules arranged in hexagonal ice phase (iceIh) is generated following Bernal-Fowler ice rules[52] and having zero net dipole moment. All simulations were run in NPT ensemble with an integration time step of 1 fs, and the Nose-Hoover thermostat[53] and barostat[54] time constant was set as 0.1 and 1 ps, respectively. At each temperature and pressure, the system was equilibrated for 1 to 2 ns. A cutoff for van der Waals interaction of 9.5 Å was used. The long range Coulomb interaction was treated with particle-particle-particle mesh (PPPM) Ewald summation[55] with a real-space cutoff of 8.5 Å. For more efficient PPPM calculations in vapor phase simulations, a larger cut-off radius (25.0 Å) is used. For each pressure, the temperatures are varied with steps of 10–20 K. Previous studies have showed that the enthalpies, entropies, and heat capacities are converged within a 20 ps 2PT sampling time with the trajectory recorded every 4 fs,[32,39] and therefore an additional 20 ps simulation after equilibration is performed for the quantum 2PT analysis using Eqs. (5a), (5b), and (10)–(11c). For comparison, we also showed the classical and quantum 1PT properties, which refer to energies calculated by applying classical (Eqs. (4a) and (4b)) and quantum harmonic (Eqs. (5a) and (5b)) weighting functions, respectively. To determine the statistical uncertainty of energies obtained from the 2PT method, we ran a 5 ns long simulation after equilibration. An additional 20 ps trajectory after each nanosecond simulation was recorded and analyzed using the 2PT method. The enthalpy standard deviation of the five 2PT runs (20 ps) is 0.01, 0.05, and 0.58 kJ/mol for solid, liquid, and gas phase, respectively. The entropy standard deviation for solid, liquid, and gas phase is 0.31, 0.31, and 2.40 J/mol K, respectively.

IV. RESULTS AND DISCUSSIONS

We here used TIP4P-Ew water as an example to illustrate the main features of water DoS in different phases (Sec. IV A) and detail the impact of quantum and diffusive effects on H and S in each phase in Sec. IV B. The comparison among difference water models and the implication for force field development to capture water phase boundary are discussed in Secs. IV C and IV D.

A. Density of states of gas, liquid, and solid water

The variation of the DoS of water with its state condition (phase) is illustrated in Figure 1(a). Note that there is no

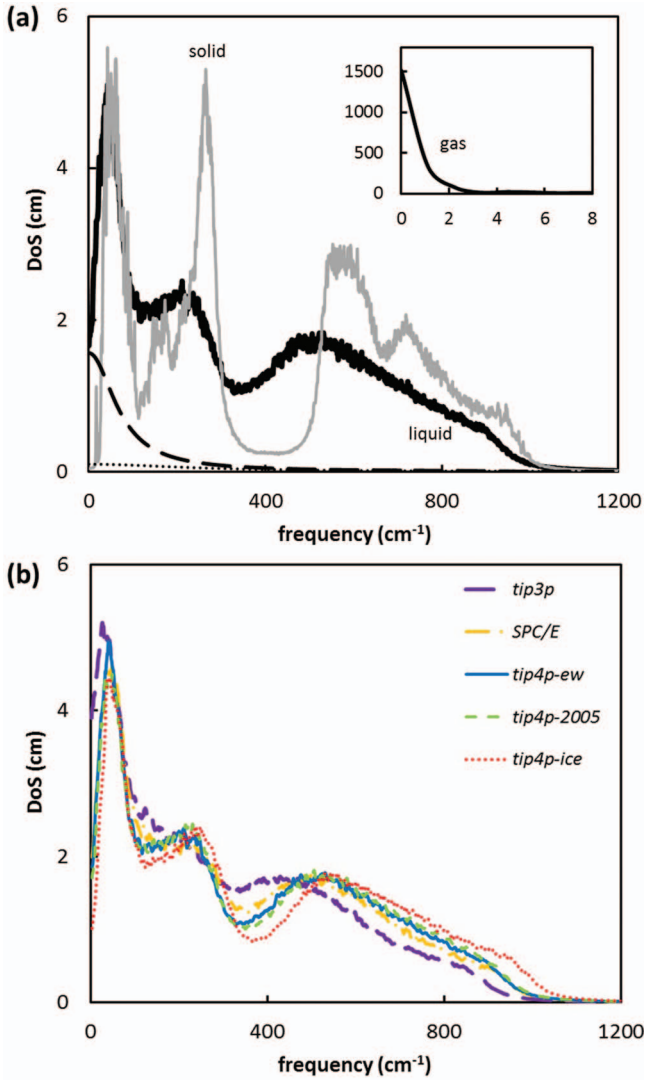

FIG. 1. (a) The density of states of TIP4P-Ew water at 1 bar and 220 K (gray solid curve, iceIh), 300 K (black solid curve, liquid), and 380 K (inset, vapor). The gas-like components for liquid water associated with translational and rotational motions are shown in long dashed and dotted curves, respectively. (b) The density of state of liquid water at 300 K and 1 bar from various water models.

internal vibrational motion from the rigid water models considered in this study and the DoS do not have the high frequency H-O-H angle bending and OH stretching modes. As noted previously, the intensity of DoS at the zero frequency represents the diffusive behavior of a system. The DoS of water vapor decays rapidly, and vanishes within frequency less than 4 cm^{-1} (inset of Fig. 1(a)). Liquid phase also shows diffusive mode at zero frequency (black solid curve) but the intensity is smaller compared to that of vapor. The 2PT method identifies the gas-like contribution to the liquid water as shown by dashed and dotted curves, for translational and rotational motions, respectively. The DoS of ice (gray solid curve) has a nearly zero value of zero-frequency intensity with prominent peaks associated with localized vibrational motions. Two peaks associated with translational motions appear at frequency less than 300 cm^{-1} while rotational peaks are located near 500 cm^{-1}. The lower frequency translational peak, located near 40 cm^{-1}, is due to the bending motion of three hydrogen bonded pair, and the high frequency one, located near 260 cm^{-1}, is due to hydrogen bond stretching.[56] The peaks in liquid phase shift toward lower frequency with less pronounced feature compared to the ice DoS because of less structured water arrangement in the liquid phase.

When compared to spectroscopic measurements of liquid water,[57] our calculated frequency associated with hydrogen bond bending at 60 cm^{-1} agrees with the experimental results (50 cm^{-1}) whereas the one associated with the hydrogen bond stretching is 80 cm^{-1} higher than the experimental measurement (260 vs. 180 cm^{-1}), as shown in Figure 1(b). The experimental result also reveals a rotational band at 650 cm^{-1} from liquid water. However, TIP3P water shows a peak near 400 cm^{-1}, and the corresponding peaks of other water models shift to 500 cm^{-1}. The frequency shifts to higher frequency region when the temperature decreases is consistent with experimental measurements. The shape of DoS functions and the competition between solid-like and gas-like weighting functions, which depend strongly on water-water interactions and water environment, determine the water thermodynamic properties.

B. Quantum and diffusive effects to the enthalpy, entropy, and heat capacity of water

The calculated enthalpies ($H = E + PV$) of TIP4P-Ew using quantum 1PT (Eqs. (3), (5a) and (5b)), quantum 2PT (Eqs. (5a), (5b) and (10)–(11c)), and classical 1PT method (Eqs. (3)–(4b)) along with the experimental values[58] at 1 bar are shown in Figure 2. For comparison, the enthalpy of water vapor at 373 K is set to be zero for all methods (reference state). In other words, the reported enthalpies shown in Figure 2 were calculated as $H(T)-H$ (373 K, vapor).

The classical 1PT results (with E^{MD} and PV determined directly from the force field for TIP4P-Ew water), identical to the energy obtained from reported classical MD simulation, overestimate the enthalpy of vaporization and melting (lower liquid and solid H compared to experiment). Quantum effects (difference between quantum and classical 1PT values) largely improve the agreement with experimental value, especially in the solid phase. Quantum effects also include the zero point energy and thus increase of value of H for solids. The difference between quantum 2PT and quantum 1PT values (diffusive effect) is found not significant for enthalpy in all three phases.

For liquid and vapor water, the temperature dependence of H is quite linear and the experimental Cp are also almost constant over a wide range of temperature.[58] For the solid phase, the H was fitted with a third-order polynomial because this expression provides a good description of experimental enthalpies of iceIh.[58]

Since the diffusive effect on H is not significant, the negligible difference between the quantum 1PT and 2PT determined Cp is expected (see Table I). The classical 1PT Cp of vapor and liquid TIP4P-Ew water are found to be too large (54 and 86 J/mol/K) compared to the experimental values (36 and 75 J/mol/K), in agreement with reported classical results using both H derivative or energy fluctuation.[59] Quantum correction correctly reduces the value of Cp (52 and 70 J/mol/K

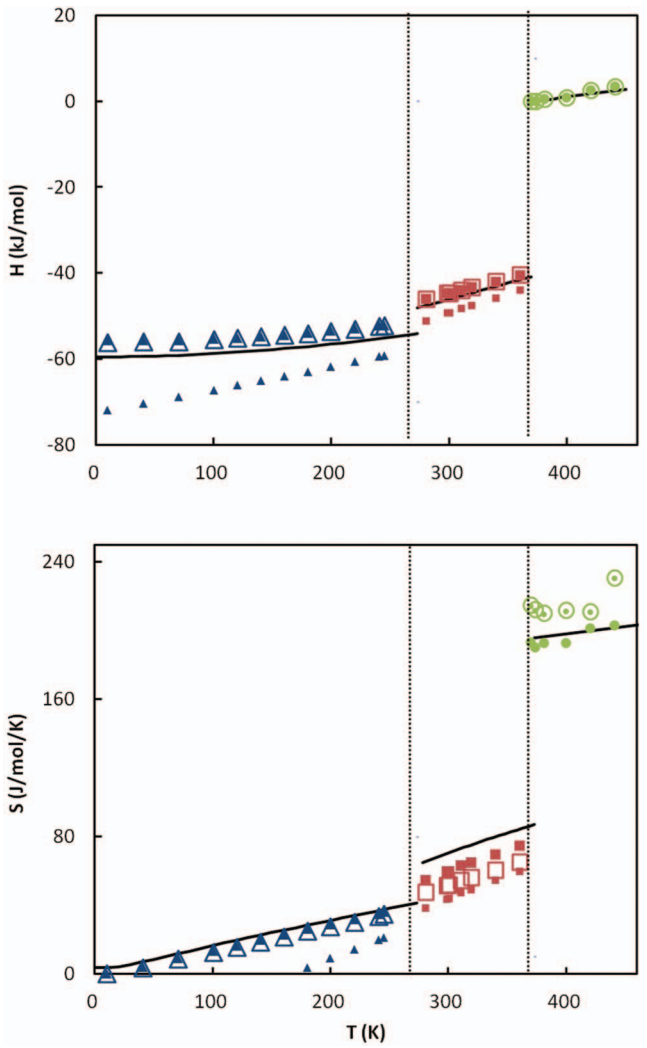

FIG. 2. Classical 1PT (small-solid symbols), quantum 1PT (empty symbols), and quantum 2PT (large-solid symbols) calculated (a) enthalpies relative to the gas enthalpy at 373 K [$H - H_{gas}$, 373 K] and (b) entropies as a function of temperature from TIP4P-Ew water. The solid lines represent experimental values.[57,58] Results of solid, liquid, and gas water are shown in triangles, squares, and circles, respectively. The dashed vertical lines represent the melting and boiling temperatures. All the simulations are done at pressure of 1 bar.

TABLE I. Comparison of calculated liquid and gas phase heat capacity (*Cp*) for different water models using the temperature derivative of classical 1PT, quantum 1PT, and quantum 2PT enthalpies at 1 bar.

	TIP3P	SPC/E	TIP4P-Ew	TIP4P-2005	TIP4P-ice
Cp, *liquid* (J/mol/K)					
Cp (quantum 2PT)	60 ± 1	68 ± 1	69 ± 1	68 ± 2	67 ± 0
Cp (quantum 1PT)	61 ± 1	65 ± 2	70 ± 0	69 ± 2	68 ± 1
Cp (classical 1PT)	86 ± 1	87 ± 1	86 ± 1	89 ± 2	88 ± 1
Cp (expt. at 300 K)[57]			75		
Cp, *vapor* (J/mol/K)					
Cp (quantum 2PT)	41 ± 3	51 ± 11	52 ± 2	47 ± 4	64 ± 12
Cp (quantum 1PT)	41 ± 2	45 ± 3	52 ± 2	45 ± 3	62 ± 11
Cp (classical 1PT)	42 ± 3	49 ± 5	54 ± 2	49 ± 5	61 ± 11
Cp (expt. at 400 K)[57]			36		

from quantum 1PT and 52 and 69 J/mol/K from quantum 2PT) and thus improve agreement with experiments. Previous studies using sophisticated path integral methods to take into account nuclei quantum effects[26] or harmonic quantum effects[59] also found the importance of quantum effects on heat capacity. Quantum effects are crucial for *Cp*, especially in the solid phase. As shown in Figure 3, the classical 1PT *Cp* remains nearly constant of 49 J/mol K (~$6k_B$), indicating that the potential energy and the lattice size of iceIh is only slightly affected by temperature variation. However, the deviation from the constant value suggests that anharmonicity plays a role even in the solid phase. In concert with Waheed and Edholm's SPC/E result obtained from the enthalpy fluctuation calculation in MD simulations[59] and path integral approach by Vega's group,[26] quantum corrected *Cp* gradually decrease to zero as the temperature approaches to absolute zero, obeying the third law of thermodynamics. Although inclusion of quantum effects show minor influence on gas H, it not only improves the absolute value of H for solid and liquid, but also their temperature dependency, highlighting the importance of taking quantum effects into account even for a fluid system with strong classical characteristics. The improved *Cp* agreement with experiments indicates the temperature dependent energy variation is captured only when the quantum effects are considered.[60] Note that since classical force fields are normally parameterized to reproduce experimental *H* of vaporization,[45–47] the simultaneous agreement in *Cp* may not be possible without consideration of quantum effects. In other words, classical force fields often fail to provide correct enthalpic properties for water over a large range of temperatures.

Both quantum and diffusive effects are important to reproduce experimental *S* for solid, liquid, and vapor water

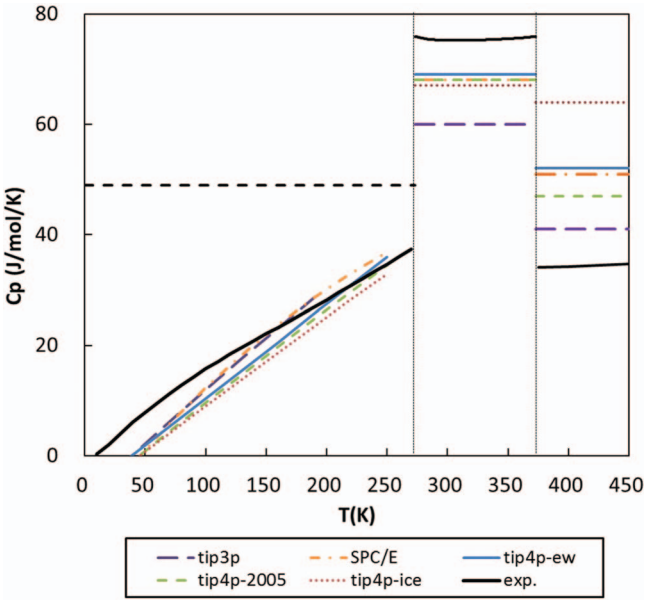

FIG. 3. The quantum 2PT calculated heat capacities (*Cp*) as a function of temperatures at 1 bar from different water models. Experimental results are shown in solid black curve.[57,58] The vertical dotted lines indicate the melting and boiling temperature, respectively, and the broken horizontal line represents the classical Cp of solid.

(Figure 2(b)). The classical 1PT values are obtained by considering each mode in the *DoS* as a classical harmonic oscillator. Since harmonic approximations are poor for diffusive modes and classical harmonic oscillator is improper at low temperatures (resulting in negative entropy, see Eq. (4b), the classical entropy is significantly overestimated for water vapor and underestimated for ice. Similar to the *H* results, the quantum effects on entropy increase with increasing solid density or decreasing temperature. The negligible quantum effects in the gas phase is due to the small difference of entropy weighting function between classical and quantum harmonic oscillators within low frequency region.[25,31] In contrast to the trivial influence of diffusive effects on *H*, the consideration of diffusive effects leads to a remarkably improved representation of water entropy. For gas phase, quantum corrected entropy (1PT) is overestimated because the vibrational modes are mostly located at low frequency region (<3 cm^{-1}), as shown in Figure 1(a), where the weighting function of harmonic oscillation is larger than the hard-sphere or ideal gas description.[31] Taking the diffusive effect into account (quantum 2PT vs quantum 1PT), *S* is increased in liquid and solid phases whereas in gas phase *S* is reduced. Considering both quantum and diffusive effects, the quantum 2PT calculated water *S* provides the best agreement with experiments for each water phase. In addition, when the quantum 2PT method is compared to more advanced thermodynamic models, the 2PT method and finite difference or free energy perturbation methods give similar water entropy results.[32] The 2PT method provides an efficient way for entropy calculations from solid, liquid to vapor phase.

C. Comparison among different water models

The performance of 5 commonly used rigid water models on reproducing the *H* of *S* is examined here. Such an analysis indicates whether a model accurately captures water hydrogen bonding network and dynamics in different environments, which are particularly difficult for condensed phases. The DoS of liquid water from various models are compared in Figure 1(b). The main DoS features are similar with minor differences. TIP3P water has the highest intensity of zero frequency and has no clear peak associated with hydrogen bond stretching (near 300 cm^{-1}). SPC/E, TIP4P-Ew, and TIP4P-2005 models have nearly indistinguishable DoS. The location of the peak associated with the rotational motion becomes more crystalline-like for TIP4P-ice, whose zero frequency intensity is also the smallest. The thermodynamic properties of each model that strongly depends on DoS features are discussed as follow.

As shown in Figures 4 and 5, all the tested water models perform reasonably well in reproducing the experimental gas *H* and *S* as well as their temperature dependency. For SPC/E, TIP4P-Ew, and TIP4P-2005 models, all of which are parameterized for liquid water and show nearly identical DoS in Figure 1(b), the liquid *H* obtained from the 2PT agrees with experiments whereas the solid *H* is slightly overestimated; liquid and solid *S* are underestimated. While the TIP3P model accurately captures solid, liquid, and gas entropies, its liquid phase diffusivity (5.25 cm^2/s at 298 K) is more than two times larger than the experimental value (2.3 cm^2/s at 298 K),[61] as shown in its high intensity of zero frequency in Figure 1(b). In addition, the liquid and solid *H* are overestimated. These results all indicate that the strength of hydrogen-bond of TIP3P water in condensed phases may be too weak, as evidenced in the lack of liquid DoS feature associated hydrogen bond stretching motion. On the contrary, TIP4P-ice, parameterized to reproduce the melting point of water by enhancing the H-bond strength,[49] leading to too low liquid diffusivity (1.33 cm^2/s at 298 K) and a blue shift of the rotational DoS peak compared to other models. The *H* and *S* of TIP4P-ice liquid water are underestimated, indicating a too structured liquid phase. These findings are consistent with Henchman's analysis based on the cell theory.[62] The comparison among different models demonstrates the strong correlation between water structure in terms of enthalpy, entropy, and diffusivity. None of the five rigid water models tested in this work successfully reproduces all these properties simultaneously.

It is noteworthy that entropies of liquid water from more sophisticated water models such as the reactive force field[63] and *ab initio* MD simulations with various density functionals[63,64] have also been reported recently. All the empirical potentials underestimate the *S* of liquid water at the ambient condition and the *S* obtained from density functionals deviates from the experiment even more. Galli and coworkers[64] attributed the underestimation obtained from commonly used functionals to overstructured liquid water, which is evidenced by the much too low diffusivity. It is shown recently that including nuclear quantum effects in the *ab initio* molecular dynamics simulations softens the structure of liquid water and improves the dynamic properties[38] and more accurate liquid water *H* and *S* might be expected.

D. Phase boundary and corresponding property changes

The knowledge of *H* and *S* can be used to identify the phase transition conditions. Under the same *T* and *P*, the more stable phase has a lowest value of Gibbs free energy, $G(=H-TS)$. In other words, at a given pressure the melting (T_m) and boiling (T_b) temperature can be determined based on the equality of *G* of the coexisting phases. Here, we fitted $G(T)$ of each phase with a second-order polynomial and analytically solved a set of simultaneous equations consisting of $G(T)$ from two different phases. Table II summarizes the T_b and T_m of various water models at pressure of 1 bar as well as *H* of vaporization at 373 K and *H* of melting at 273 K based on classical 1PT, quantum 1PT, and quantum 2PT enthalpy and entropy. Note that the phase transition conditions can also be obtained by directly simulating the coexisting phases (one infinite slab for each phase),[65] Gibbs ensemble Monte Carlo (GEMC),[66,67] and Hamiltonian Gibbs-Duhem integration.[21] The transition condition determined via two-phase coexisting models is noted as "direct" phase boundary in Table II.

Enthalpies and entropies have competing contributions to free energies and thus have opposite effect on the

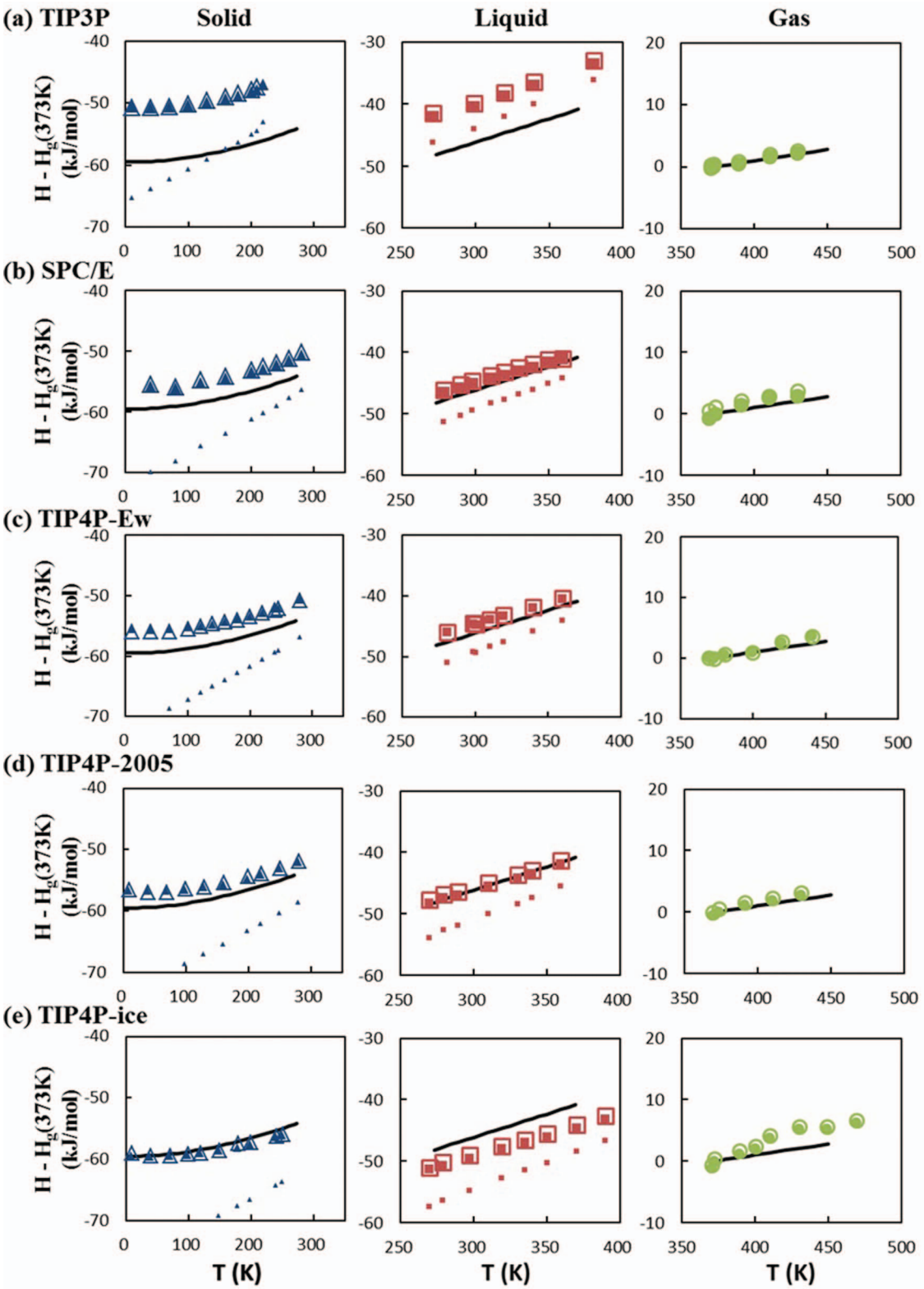

FIG. 4. Classical 1PT (small-solid symbols), quantum 1PT (empty symbols), and quantum 2PT (large-solid symbols) calculated enthalpies relative to the gas enthalpy at 373 K [$H - H_{gas}$, 373 K] as a function of temperature from various water models. The solid lines represent experimental enthalpies. The columns from the left to right are water enthalpies in solid, liquid, and gas phases. All the simulations are done at pressure of 1 bar. The enthalpy standard deviation for solid, liquid, and gas phase is 0.01, 0.05, and 0.58 kJ/mol, respectively.

determined equilibrium temperature. As shown in Table II, both quantum and classical 2PT models provide better agreement of T_b than 1PT models, compared to the experiments. T_b is increased from quantum 2PT to classical 2PT model. The classical and quantum 1PT predicted T_b is 10–40 K lower than the quantum 2PT calculated value due to the overestimation of gas phase entropy and the underestimation of liquid entropy. Although the classical 2PT determined T_b

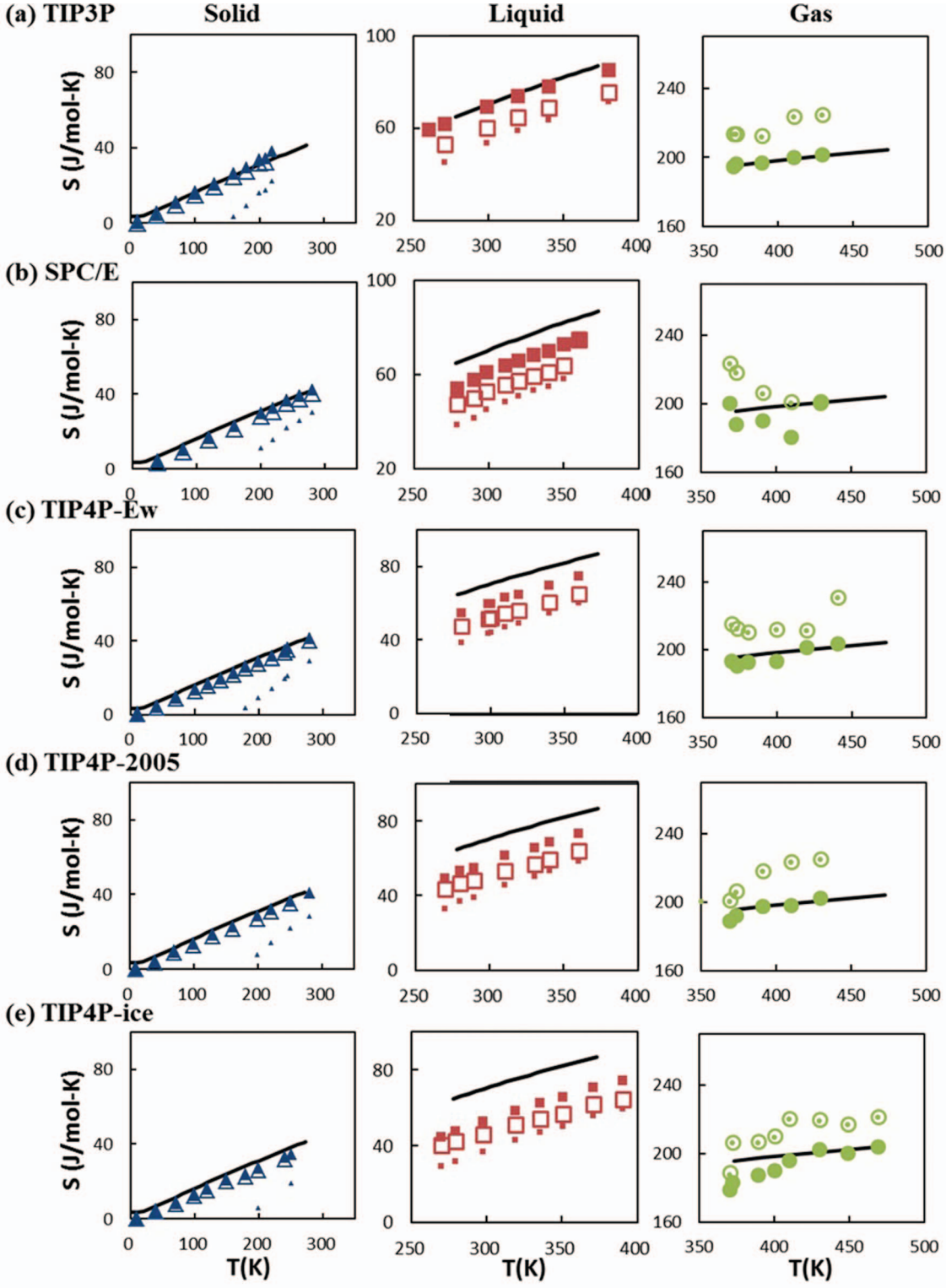

FIG. 5. Classical 1PT (small-solid symbols), quantum 1PT (empty symbols), and quantum 2PT (large-solid symbols) calculated entropies as a function of temperature from various water models. The solid lines are experimental enthalpies. The columns from the left to right are solid, liquid, and gas entropies. All the simulations are done at pressure of 1 bar. The entropy standard deviation for solid, liquid, and gas phase is 0.31, 0.31, and 2.40 J/mol K, respectively.

provides the highest T_b among these four approaches, the T_b is still lower than those from Gibbs-Duhem simulations by 30 K. The TIP3P model, which has the smallest heat of vaporization at 373 K and the most accurate entropy change, shows the lowest T_b, in concert with its high diffusive behavior. Among the TIP4P-series models, the predicted T_b gradually increases from TIP4P-Ew to TIP4P-ice model, in agreement with the results from the Gibbs-Duhem simulations[70] although the quantum 2PT results are 45–70 K lower, and classical 2PT results are 30 K lower. The 2PT methods and Gibbs-Duhem simulations determined G are expected to be similar, indicating that the 2PT method tends to provide less

TABLE II. Comparison of the heat of vaporization (373 K) and melting (273 K) in kJ/mol at 1 bar as well as the free energy determined boiling (T_b) and melting (T_m) temperatures in K for different water models using classical 1PT, quantum 1PT, classical 1PT, and quantum 2PT approach.

	TIP3P	SPC/E	TIP4P-Ew	TIP4P-2005	TIP4P-ice
373 K, 1 bar					
ΔH (2PT quantum)	35.46	40.19	40.10	41.03	43.72
ΔH (1PT quantum)	35.40	40.72	39.54	41.29	44.34
ΔH (1PT classical)	38.25	43.69	42.78	44.51	48.17
ΔH (expt.)			40.6		
T_b (2PT quantum)	324	361	336	358	392
T_b (2PT classical)	339	372	359	372	407
T_b (1PT quantum)	290	349	327	349	352
T_b (1PT classical)	299	353	324	353	356
T_b (*Gibbs-Duhem simulations*)[70,a]			394	*401*	*437*
273 K, 1 bar					
ΔH (2PT quantum)	N/A[b]	3.86	4.50	4.41	4.34
ΔH (1PT quantum)	N/A[b]	4.02	4.66	4.71	4.46
ΔH (1PT classical)	N/A[b]	4.95	5.68	5.64	5.40
ΔH (expt.)			6.0		
T_m (2PT quantum)	217	310	324	336	356
T_m (2PT classical)	246	346	345	362	393
T_m (1PT quantum)[c]	284	390	380	439	448
T_m (1PT classical)[c]	...	443	396	428	488
T_m (direct)[65,d]	*147*[e]	213	242	249	268

[a]Vapor-liquid equilibria computed using Gibbs-Duhem simulations.
[b]No stable or meta-stable solid phase at 273 K.
[c]IceIh melts at the classical and 1PT free energy determined T_m.
[d]Melting condition obtained from simulating two coexisting phases in MD simulation.
[e]Melting temperature obtained from the thermodynamic integration approach.[68]

stable liquid phase (more positive G) compared to the Gibbs-Duhem simulation, which also affects the T_m determination and the shape of the water phase diagram.

The difficulty to accurately predict T_m emphasizes the inability of rigid water model to simultaneously capture hydrogen bonding network of solid and liquid. We here focus on TIP4P-series models because iceIh melts into liquid state during the NPT simulation when the temperature is higher than 240 K for TIP3P model.[68,69] The quantum 2PT method overestimates the T_m by 50–80 K versus experiments and 80–90 K versus the direct coexistence simulation, as shown in Table II. The classical 2PT T_m is even higher than the quantum 2PT values. Although T_m obtained from Gibbs-Duhem integration is consistent with the solid-liquid interfacial simulation, the chemical potentials of iceIh and liquid are calculated based on different thermodynamic approximation.[21] The 2PT determined T_m is slightly above (∼5 K) the temperature where the solid ice melts into liquid water during the simulation. The overestimation of T_m from quantum 2PT determined G is consistent with that obtained from the cell theory,[62] where the same treatment is applied to both solid and liquid phases. The classical 1PT predicted T_m occurs at higher temperatures where the crystalline water melts into liquid during the simulation. Although the classical 1PT and classical 2PT models provide similar G of ice phase, the decrease of liquid G from the 2PT classical model leads to a lower T_m compared to the 1PT classical model. The large deviation in T_m compared to experiments is mainly due to the underestimation of liquid phase entropy. Although the quantum 2PT calculated heat of melting of these TIP4P-series water models is ∼2 kJ/mol smaller compared to the experiments (see Table II), the entropic contribution (TS) to the free energy change at 273 K is still not large enough to reach free energy equality. The predicted T_m strongly depends on the value of liquid entropy. The smaller the liquid entropy is, such as TIP4P-ice, the higher the T_m will be. In Table II, the predicted T_m value is in the order of TIP4P-ice > TIP4P-2005 > TIP4P-Ew. This trend is also consistent with quadrupole moment variation trend of water models. TIP4P-ice, which has the largest quadrupole moment, gives rather high melting point.[69] The relationship has also been noticed for the cases when T_m are determined using direct coexistence simulations, suggesting that the 2PT calculated T_m still follows the results from interfacial simulations and just shift the melting curve to a higher temperature range.

A direct comparison between the quantum 2PT results and the path integral simulation is difficult due to the use of different water potentials but the influence of quantum effect on T_m from both methods is consistent. The T_m from quantum path integral simulation using the TIP4PQ/2005 potential is 257 K, compared to 282 K obtained from its classical counterpart.[71] The decrease of T_m from classical to quantum approach is consistent with our results (quantum 2PT/1PT vs. classical model) although all of our calculations overestimate the T_m.

We further extended our simulations at pressure other than 1 bar and carried out the calculations to explore the overall water phase diagram. Figure 6 shows the phase diagram of

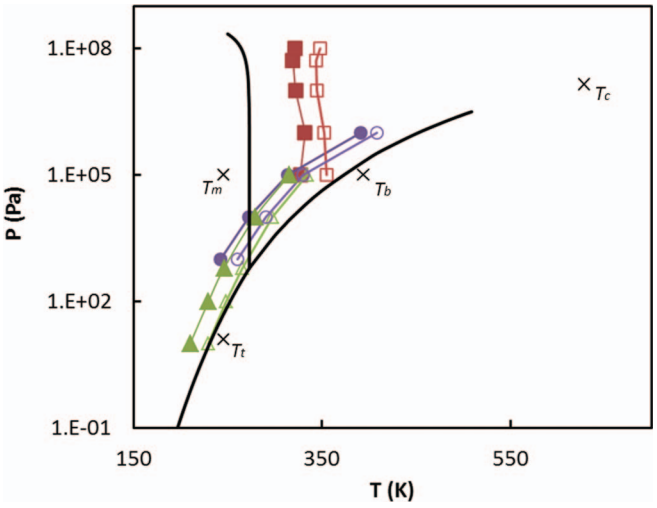

FIG. 6. Phase diagram of TIP4P-Ew water as obtained from experimental (black-solid lines), from the quantum 2PT (filled symbols), and classical 1PT (empty symbols) free energy calculations. The melting (T_m), boiling (T_b), critical (T_c), and triple (T_t) point computed using Gibbs-Duhem simulations[70] (cross symbols) are also shown for comparison. Melting, vaporization, and sublimation points are shown in red squares, purple circles, and green triangles, respectively. Connecting lines are used for guiding the eye.

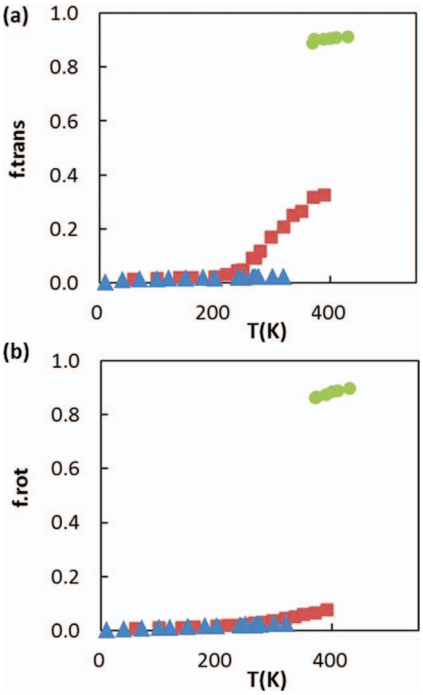

FIG. 7. The 2PT calculated (a) translational and (b) rotational fluidicity of TIP4P-ice water as a function of temperature at 1 bar for solid (triangles), liquid (squares), and vapor (circles) phases.

TIP4P-Ew water. The quantum 2PT calculated phase boundary is qualitatively consistent with experiments. As discussed in the 1 bar case (Table II), the temperature range where the liquid phase exists (T_b–T_m) is squeezed from quantum 2PT. This range is even squeezed from classical 2PT. When compared to experimental phase diagram, the calculated melting curves shift to higher temperature region whereas the boiling curve slightly shifts to low temperature region, in contrast to thermodynamic integration results in which the boiling temperature is enhanced[70] and the melting temperature is reduced,[21] also shown in Fig. 6. The sublimation curve fairly agrees with the experiment. The shifts of melting and boiling curves might be attributed to a less stable (large H and small S) liquid phase, partially due to strong quantum effect considered in the quantum 2PT method. The lack of considerations of H and S interrelation and the influence of quantum effect in the force field development are also responsible for the water phase boundary deviation.

E. Temperature dependency of fluidicity of water in different states of matter

The fluidicity, as calculated from Eq. (8), is the key variable in the 2PT theory that separates the diffusive degrees of freedom from the non-diffusive ones. Figure 7 illustrates the temperature dependency of the translational and rotational fluidicity of TIP4P-ice water at 1 bar for the vapor (circle), liquid (square), and solid (triangle) phases. As expected, both f_{trans} and f_{rot} increase with increasing temperature, reflecting the more important influence of diffusive effects. Temperature leads to most significant influence on the fluidicity for liquid phase than other two phases.

The temperature dependent liquid fluidicity also reveals an important aspect of water dynamics in the phase transition. At low temperatures, the translational and rotational fluidicity of liquid phase nearly overlaps with the solid phase (which remains approximately zero) and starts increasing near 270 K, which is consistent with the melting point, T_m, obtained from liquid-solid interface simulation.[65] We have examined the temperature dependence of fluidicity for other water models and found similar results (not shown). As the water enters the vapor phase condition, the fluidicity reaches a plateau. Therefore, the temperature variation of the fluidicity of liquid water can be a simple indicator for phase transition.

V. CONCLUSION

The 2PT method allows for effective calculation of water H and S in all possible states of matter from MD simulations. Therefore, it can be a useful tool for exploring the role of water in biological systems or nano-confinements where its state of aggregation may not be always clear. In addition, an important 2PT parameter fluidicity, f_{trans}, that defines the proportion of gas-like and solid-like properties also provides a fast way to investigate liquid water dynamic properties corresponding to the phase transition.

Quantum effects are important for accurate description of heat capacity and enthalpy of ice and liquid water, whereas consideration of gas-like component is critical for entropy of liquid and vapor water. In other words, both quantum and the diffusive properties are important to capture the properties of liquid water.

In the 2PT theory, water structure (represented by its DoS) and diffusivity (represented by fluidicity) directly influence the value of H and S and the interplay of these properties are difficult to capture using a simple rigid water model.

Although the 2PT model improves H and S values from these empirical models, the deviation from experiments still leads to large deviation of water melting and vaporizing temperatures. Our results indicate that water interactions described by force fields still dominate thermodynamic properties and it is rather difficult to accurately model *H* and *S* of water simultaneously over a wide range of temperature. While conventional parameterization of classical water model only aims to reproduce experimental enthalpies, the 2PT method might provide an effective way to take into account *H* and *S* simultaneously for an improved water force field.

ACKNOWLEDGMENTS

This research was partially supported by the National Science Council (102-3113-P-002-01), Ministry of Economic Affairs (102-5226904000-05-03), and Ministry of Education (102R4000) of Taiwan. The computation resources from the National Center for High-Performance Computing of Taiwan and the Computing and Information Networking Center of the National Taiwan University are acknowledged.

[1]P. Kebarle, S. K. Searles, A. Zolla, J. Scarboro, and M. Arshadi, J. Am. Chem. Soc. **89**, 6393 (1967).
[2]R. Lumry and S. Rajender, Biopolymers **9**, 1125 (1970).
[3]Z. Shi, J. V. Ford, S. Wei, and A. W. Castleman, J. Chem. Phys. **99**, 8009 (1993).
[4]V. P. Denisov, K. Venu, J. Peters, H. D. Horlein, and B. Halle, J. Phys. Chem. B **101**, 9380 (1997).
[5]A. Scala, F. W. Starr, E. La Nave, F. Sciortino, and H. E. Stanley, Nature **406**, 166 (2000).
[6]Y. Harano and M. Kinoshita, Chem. Phys. Lett. **399**, 342 (2004).
[7]S. T. Lin, P. K. Maiti, and W. A. Goddard, J. Phys. Chem. B **109**, 8663 (2005).
[8]B. Jana, S. Pal, P. K. Maiti, S. T. Lin, J. T. Hynes, and B. Bagchi, J. Phys. Chem. B **110**, 19611 (2006).
[9]D. H. Leung, R. G. Bergman, and K. N. Raymond, J. Am. Chem. Soc. **130**, 2798 (2008).
[10]A. Debnath, B. Mukherjee, K. G. Ayappa, P. K. Maiti, and S. T. Lin, J. Chem. Phys. **133**, 174704 (2010).
[11]B. Nandy and P. K. Maiti, J. Phys. Chem. B **115**, 217 (2011).
[12]B. J. Borah, P. K. Maiti, C. Chakravarty, and S. Yashonath, J. Chem. Phys. **136**, 174510 (2012).
[13]B. Breiten, M. R. Lockett, W. Sherman, S. Fujita, M. Al-Sayah, H. Lange, C. M. Bowers, A. Heroux, G. Krilov, and G. M. Whitesides, J. Am. Chem. Soc. **135**, 15579 (2013).
[14]V. A. Sirotkin and A. V. Khadiullina, J. Chem. Phys. **139**, 075102 (2013).
[15]A. Debnath, K. G. Ayappa, and P. K. Maiti, Phys. Rev. Lett. **110**, 018303 (2013).
[16]T. A. Pascal, W. A. Goddard, P. K. Maiti, and N. Vaidehi, J. Phys. Chem. B **116**, 12159 (2012).
[17]H. Kumar, B. Mukherjee, S.-T. Lin, C. Dasgupta, A. K. Sood, and P. K. Maiti, J. Chem. Phys. **134**, 124105 (2011).
[18]L. Jensen, K. Thomsen, N. von Solms, S. Wierzchowski, M. R. Walsh, C. A. Koh, E. D. Sloan, D. T. Wu, and A. K. Sum, J. Phys. Chem. B **114**, 5775 (2010).
[19]D. Frenkel and B. Smit, *Understanding Molecular Simulation: From Algorithms to Applications* (Academic Press, New York, 2002).
[20]R. H. Henchman, J. Chem. Phys. **126**, 064504 (2007).
[21]C. Vega, E. Sanz, J. L. F. Abascal, and E. G. Noya, J. Phys.: Condens. Matter **20**, 153101 (2008).
[22]J. G. Kirkwood, J. Chem. Phys. **3**, 300 (1935).
[23]M. S. Wertheim, J. Stat. Phys. **35**, 35 (1984).
[24]B. Widom, J. Chem. Phys. **39**, 2808 (1963).
[25]P. H. Berens, D. H. J. Mackay, G. M. White, and K. R. Wilson, J. Chem. Phys. **79**, 2375 (1983).
[26]C. Vega, M. M. Conde, C. McBride, J. L. F. Abascal, E. G. Noya, R. Ramirez, and L. M. Sese, J. Chem. Phys. **132**, 046101 (2010).
[27]D. A. McQuarrie, *Statistical Mechanics* (University Science Books, 2000).
[28]P. Debye, Ann. Phys. **344**, 789 (1912).
[29]B. Bagchi, Chem. Rev. **105**, 3197 (2005).
[30]N. Nandi and B. Bagchi, J. Phys. Chem. B **101**, 10954 (1997).
[31]S. T. Lin, M. Blanco, and W. A. Goddard, J. Chem. Phys. **119**, 11792 (2003).
[32]S. T. Lin, P. K. Maiti, and W. A. Goddard, J. Phys. Chem. B **114**, 8191 (2010).
[33]P.-K. Lai, C.-M. Hsieh, and S.-T. Lin, Phys. Chem. Chem. Phys. **14**, 15206 (2012).
[34]B. J. Berne and D. Thirumalai, Annu. Rev. Phys. Chem. **37**, 401 (1986).
[35]L. H. de la Pena, M. S. G. Razul, and P. G. Kusalik, J. Chem. Phys. **123**, 144506 (2005).
[36]L. H. de la Pena and P. G. Kusalik, J. Am. Chem. Soc. **127**, 5246 (2005).
[37]C. McBride, C. Vega, E. G. Noya, R. Ramirez, and L. M. Sese, J. Chem. Phys. **131**, 024506 (2009).
[38]F. Paesani and G. A. Voth, J. Phys. Chem. B **113**, 5702 (2009).
[39]S.-N. Huang, T. A. Pascal, W. A. Goddard III, P. K. Maiti, and S.-T. Lin, J. Chem. Theory Comput. **7**, 1893 (2011).
[40]C. Caleman, P. J. van Maaren, M. Y. Hong, J. S. Hub, L. T. Costa, and D. van der Spoel, J. Chem. Theory Comput. **8**, 61 (2012).
[41]M. P. Desjarlais, Phys. Rev. E **88**, 062145 (2013).
[42]J. Han, W. Y. Wang, C. Wang, Y. Wang, X. Liu, and Z.-K. Liu, Fluid Phase Equilib. **360**, 44 (2013).
[43]J. Wang, B. Chakraborty, and J. Eapen, Phys. Chem. Chem. Phys. **16**, 3062 (2014).
[44]C. Vega and J. L. F. Abascal, Phys. Chem. Chem. Phys. **13**, 19663 (2011).
[45]W. L. Jorgensen, J. Chandrasekhar, J. D. Madura, R. W. Impey, and M. L. Klein, J. Chem. Phys. **79**, 926 (1983).
[46]H. J. C. Berendsen, J. R. Grigera, and T. P. Straatsma, J. Chem. Phys. **91**, 6269 (1987).
[47]H. W. Horn, W. C. Swope, J. W. Pitera, J. D. Madura, T. J. Dick, G. L. Hura, and T. Head-Gordon, J. Chem. Phys. **120**, 9665 (2004).
[48]J. L. F. Abascal and C. Vega, J. Chem. Phys. **123**, 234505 (2005).
[49]J. L. F. Abascal, E. Sanz, R. G. Fernandez, and C. Vega, J. Chem. Phys. **122**, 234511 (2005).
[50]N. F. Carnahan and K. E. Starling, J. Chem. Phys. **53**, 600 (1970).
[51]S. Plimpton, J. Comput. Phys. **117**, 1 (1995).
[52]J. D. Bernal and R. H. Fowler, J. Chem. Phys. **1**, 515 (1933).
[53]W. G. Hoover, Phys. Rev. A **31**, 1695 (1985).
[54]W. G. Hoover, Phys. Rev. A **34**, 2499 (1986).
[55]T. Darden, D. York, and L. Pedersen, J. Chem. Phys. **98**, 10089 (1993).
[56]Y. Koyama, H. Tanaka, G. T. Gao, and X. C. Zeng, J. Chem. Phys. **121**, 7926 (2004).
[57]G. E. Walrafen, M. R. Fisher, M. S. Hokmabadi, and W. H. Yang, J. Chem. Phys. **85**, 6970 (1986); H. R. Zelsmann, J. Mol. Struct. **350**, 95 (1995).
[58]M. Cho, G. R. Fleming, S. Saito, I. Ohmine, and R. M. Stratt, J. Chem. Phys. **100**, 6672 (1994); R. Feistel and W. Wagner, J. Phys. Chem. Ref. Data **35**, 1021 (2006).
[59]Q. Waheed and O. Edholm, J. Chem. Theory Comput. **7**, 2903 (2011).
[60]L. H. de la Pena and P. G. Kusalik, J. Chem. Phys. **125**, 054512 (2006).
[61]M. Holz, S. Heil, and A. Sacco, Phys. Chem. Chem. Phys. **2**, 4740 (2000).
[62]M. Klefas-Stennett and R. H. Henchman, J. Phys. Chem. B **112**, 9769 (2008).
[63]T. A. Pascal, D. Scharf, Y. Jung, and T. D. Kuhne, J. Chem. Phys. **137**, 244507 (2012).
[64]C. Zhang, L. Spanu, and G. Galli, J. Phys. Chem. B **115**, 14190 (2011).
[65]R. G. Fernandez, J. L. F. Abascal, and C. Vega, J. Chem. Phys. **124**, 144506 (2006).
[66]M. Lisal, W. R. S. William, and I. Nezbeda, Fluid Phase Equilib. **181**, 127 (2001).
[67]Z. H. Duan, N. Moller, and J. H. Weare, J. Phys. Chem. B **108**, 20303 (2004).
[68]C. Vega and J. L. F. Abascal, J. Chem. Phys. **123**, 144504 (2005).
[69]J. L. F. Abascal and C. Vega, Phys. Chem. Chem. Phys. **9**, 2775 (2007).
[70]C. Vega, J. L. F. Abascal, and I. Nezbeda, J. Chem. Phys. **125**, 034503 (2006).
[71]C. McBride, E. G. Noya, J. L. Aragones, M. M. Condea, and C. Vega, Phys. Chem. Chem. Phys. **14**, 10140 (2012).